

Corrosion studies of organodithiol/monothiol derived self assembled monolayer on copper substrate towards corrosion protection in 0.5 M NaCl

S S Pathak^a, V Yegnamaran^b, J Mathiyarasu^b, M Maji^c & A S Khanna^{a*}

^aCorrosion Science and Engineering, IIT Bombay, Mumbai 400 076, India

^bEEC Division, Central Electrochemical Research Institute, Karaikudi 630 006, India

^cDepartment of Chemistry, NIT Durgapur, Durgapur 713 209, India

Email: khanna@met.iitb.ac.in

Received 2 March 2006; revised received 23 August 2006; accepted 14 September 2006

The corrosion resistance of 1-decanthiol (DT), 1,9-nonanedithiol (NDT) and 1,4-benzendimethanethiol (BDMT) self assembled monolayer (SAM) covered copper were investigated using several electrochemical methods including polarization studies and electrochemical impedance spectroscopy (EIS) in aqueous 0.5 M NaCl solution. The SAM covered surface was characterized by Fourier transform infrared reflectance spectroscopy (FTIR), atomic force microscopy (AFM) and cyclic voltammetry. The inhibition efficiency (IE) of the SAM/copper was investigated by varying: concentration of thiol in solution used for self assembly, assembly period for the formation of SAM and effect of solvents (DMF, toluene, ethanol and acetonitrile) for preparing the thiol solution. The inhibition efficiency of the different thiol compounds under similar experimental conditions for copper corrosion was found to be in the following order: NDT > DT > BDMT. The concentration of thiol and self assembly period affect the quality significantly. At the higher concentration, the self assembled monolayer was formed immediately after the solution was introduced to a substrate. There was only a marginal effect of using different solvent for dissolving the thiols on the inhibition efficiency (IE). FTIR and AFM confirm the self assembling of thiols on copper surface.

Keywords: Self assembled monolayer (SAM), Corrosion resistance, Dithiol, Copper

IPC Code: C23F11/00, C23F13/08

Due to high thermal and electrical conductivities and low cost, copper finds applications in fabricating PCBs establishing intercontacts which are crucial for the effective functioning of electronic equipments. However, copper corrodes easily under the combined effect of water (moisture), ionic dust and gases like SO₂, NO₂, HCl, Cl₂. Conventional methods of corrosion protection are often not suitable for meeting the requirements of emerging electronics industry. In the emerging scenario of microelectronics, the copper components will be in mm and (m sizes and will be requiring the protective coating to combat corrosion. These coatings are expected to be of size in the range of fraction of micron or nanosize^{1,2}. The formation of organic coatings with a well-defined thickness in the nanometer range is generally quite expensive.

Self assembled monolayer (SAM) offers a simple method to get a monomolecular film in nanometer range. SAM formation needs a very small quantity of organic corrosion inhibitor, which is economically very attractive and eco-friendly. SAM of organosulphur compounds are expected to function as

a barrier to prevent the permeation of corrosion accelerants such as moisture and electrolytes into the copper substrate, thereby improving the corrosion resistance of the copper³⁻⁵. It improves the interaction between first monolayer of inhibitor and copper by chemisorption. It has therefore become an interesting pretreatment of surface before applying of organic coating⁶. Widespread examples are alkanethiol monolayer⁷⁻¹³, silane^{14,15}/alkylisocyanate¹⁶ modified alkanethiol monolayer, Schiff base monolayer^{17,18}, and *N*-vinylcarbazole monolayer¹⁹ on oxide free copper.

Laibins and Whitesides⁴ investigated the corrosion resistance of *n*-alkanethiol monolayer covered copper in atmosphere under ambient conditions. Ma *et al.*¹² studied the influence of carbon chain length and assembly period on corrosion protection ability of alkanethiol monolayer to the underlying copper. Zamborini *et al.*¹⁰ investigated the effect of aromatic and linear chain thiol adsorbates on the oxidation of underpotentially deposited copper on gold in HClO₄ containing electrolyte solutions. The results show that aromatic SAM was found to passivate the copper

surface more effectively than linear chain SAM of equal thickness. Tan *et al.*²⁰ investigated the effect of ring substituents ($-\text{CH}_3$, $-\text{CH}(\text{CH}_3)_2$, NH_2 , $-\text{NHCOCH}_3$, $-\text{F}$) on the protective properties of self-assembled benzenethiols on copper. However, little known about the corrosion resistance of dithiol derived SAM against corrosion of copper in aggressive electrolyte.

In this article, the results of studies on the corrosion resistance properties of 1-decanethiol (DT), 1,9-nonanedithiol (NDT), and 1,4-benzenedimethanethiol (BDMT) derived SAM on copper using potentiodynamic polarization measurement, cyclic voltammetry and electrochemical impedance spectroscopy have been presented. SAM modified copper surface were characterize using atomic force microscopy (AFM) and FT-IR. Reflectance spectroscopy (FTIR).

This selection of these compounds is motivated by three reasons. First, dithiols are considered to be better SAM forming property than monothiols. Moreover, no considerable work has been reported in literature which deals with the influence of dithiol derived SAM on corrosion resistance of copper. The aim of the present study is to compare the effect of the concentration of thiol solution, self assembly period and effect of solvent on their significant effect on the SAM forming property and in turn in corrosion process.

Experimental Procedure

Chemicals and Method

1-Decanethiol (DT) (96%), 1,4-benzenedimethanethiol (BDMT) (98%), 1,9-nonanedithiol (NDT) (98%) were obtained as high grade commercial reagents from Sigma-Aldrich. Absolute ethanol, toluene (GR), *N,N*-dimethylformamide (GR) (DMF) and acetonitrile (E-Merck) were used as solvents for preparing thiol solutions of required concentration. The molecular structures of the thiols are given in Fig. 1. Sodium chloride (Qualignen), nitric acid (69%) (Merck) of analytical reagent grade and deionized water (Millipore[®] 18 M Ω) were used for preparing the electrolyte solutions.

Electrode preparation and SAM modification

A copper rod (99.8% purity) with cross-sectional area of 0.126 cm² embedded in epoxy resin mould (from Aldrich) leaving its circular cross-section only exposed to electrolyte was fabricated and used for

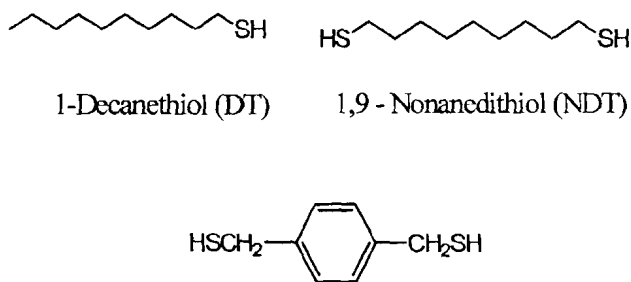


Fig. 1 — Chemical structure of thiols

electrochemical measurements. The copper used for AFM and FT-IR reflectance spectroscopy was a copper foil of same purity. The electrode surface was polished with emery paper (No. 1 to 4), ultrasonically cleaned in the solvent used for preparation of thiol solution, dried in a stream of compressed air and then etched in a 7 M HNO_3 solution for 5 s. The etched specimen was rinsed twice with deionised water, rapidly followed by rinsing with solvent and then immediately immersed in the thiol solution for SAM formation.

Electrochemical measurement

A three-electrode glass cell equipped with a platinum counter electrode, a saturated calomel reference electrode (SCE) and the fabricated copper working electrode (with or without SAM modification) was used for the electrochemical measurements. Electrochemical measurement were performed under extreme environmental condition, consisting of an aqueous, air exposed sodium chloride (0.5 M NaCl) solution.

Potentiodynamic polarization and cyclic voltammetric experiments were performed using a Potentiostat-Galvanostat Auto lab PGSTAT-30 (Eco-Chemie.V, The Netherlands). Electrochemical impedance spectroscopy (EIS) studies were performed using Solatron SI 1260, Impedance gain phase analyzer coupled with EG&G PAR Potentiostat-Galvanostat Model 273. The potentiodynamic polarization measurements were taken within the range of -0.4 to 0 V versus SCE at a rate of 0.01 V/s. Cyclic voltammetry (CVs) measurement were carried out at a scan rate of 20 mV/s in the potential rang of -0.80 to 0.80 V versus SCE in aqueous solution of 0.5 M NaCl.

EIS measurements were performed at the corrosion potentials in the frequency range from 10 kHz to 10 MHz with eight points per decade under excitation

of a sinusoidal wave of ± 5 mV amplitude. The impedance data were analyzed with the powersuit impedance software and fitted to the appropriate equivalent circuits. The fitting results gave the values of elements in the equivalent circuits.

Surface characterization of SAM modified copper surface

Atomic force microscopy

SAM modified copper surfaces were characterized by PicoSPM Atomic Force Microscopy (Molecular Imaging, USA) operated in contact mode. SiN₃ cantilever (Force constant 0.12 N/m) was used as the force sensor and the probe tip radius of curvature was about 5-10 nm. The measurement was made with the "small" 6 μ m piezoelectric z-scanner (Molecular Imaging) which was calibrated using calibration gratings supplied by the Molecular Imaging.

FT-IR reflectance spectroscopy

The transmittance FT-IR spectra of the SAM modified copper surface substrate were measured using specular reflectance accessory at 60° angle. All spectra were recorded between 4000 and 400 cm⁻¹ wave numbers using Nexus 670 FTIR spectrometer (Thermo Nicolet) equipped with a DTGS detector and averaging of 128 scans. Spectral resolution was 4 cm⁻¹. Data point resolution was approximately one point per wave number. The digitized spectra were processed using OMNIC software. To minimize problems arising from unavoidable base line shifts and to enhance the resolution of superimposed bands, the smoothed first and second derivatives of the original spectra.

Results and Discussion

Polarization and impedance studies

Corrosion behaviour of copper in 0.5 M NaCl solution

The main reactions during the corrosion of copper in an aqueous solution are anodic dissolution of copper ($\text{Cu} \rightarrow \text{Cu}^{2+} + 2\text{e}^-$) and cathodic reduction of oxygen ($\text{O}_2 + 2\text{H}_2\text{O} \rightarrow 4\text{OH}^-$). Figure 2 shows the potentiodynamic polarization curve of bare copper electrode in 0.5 M NaCl solution at 0.01 Vs⁻¹. The anodic Tafel slope (b_a) in active dissolution region is about 67.85 mv/decade which may be due to the formation of CuCl^{21,22} film. The CuCl film has poor adhesion, is unable to protect the copper surface and converts to soluble CuCl₂^{23,24} by reacting with excess chloride.

The cathodic polarization curve gave a linear region with 214.2 mV per decade slope in the potential range between -0.340 to -0.270V. The oxidants in NaCl solutions are dissolved oxygen and hydrogen ions. The reduction of dissolved oxygen is cathodic reaction here as the reduction of hydrogen ions will occur at -660 mV (versus SCE) or more negative potentials according to Nernst equation. The cathodic reaction has been proved to be diffusion controlled. A small hump observed in the cathodic curves at the potential around -0.360 may be due to reduction of CuCl.

Behavior of SAM modified copper electrode in 0.5 M NaCl

The oxide free copper electrodes were immersed in DT, NDT and BMDT toluene solutions for two hours. The polarization behavior of the SAM covered electrodes in 0.5 M NaCl at 0.01 Vs⁻¹ are given in Fig. 3. The DT SAM shifts the corrosion potential

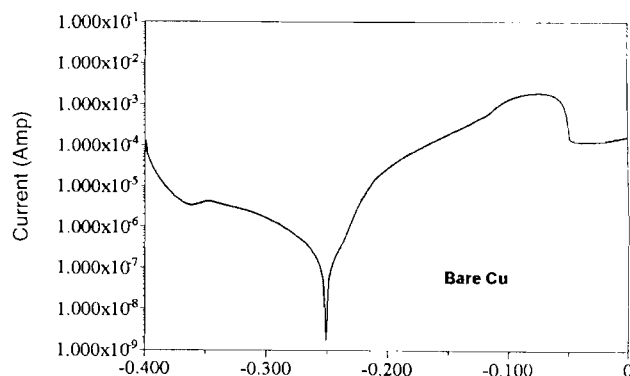


Fig. 2 — Potentiodynamic polarization of bare copper in 0.5 M NaCl solution at 0.01 Vs⁻¹

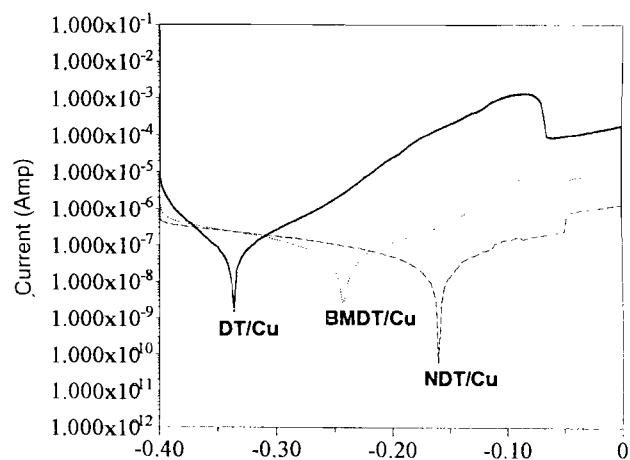


Fig. 3 — Potentiodynamic polarization of SAM modified copper with self-assembly period of two hours in 0.5 M NaCl solution at 0.01 Vs⁻¹

significantly in the cathodic direction while NDT SAM shifts it marginally to the anodic side. In the case of BDMT, SAM formation appears to have no effect on corrosion potential. However, in all the cases, the presence of SAM on the copper surface lowers the corrosion current density appreciably in comparison to bare copper. The inhibition efficiency (IE) of SAM modified copper surface is calculated from the following formula

Inhibition efficiency (IE) of SAM (%) =

$$(i_{\text{corr}} - i'_{\text{corr}}) (100) / i_{\text{corr}}$$

where i_{corr} and i'_{corr} represent the corrosion current densities of the bare and SAM-modified copper electrodes, respectively. Values of i_{corr} and i'_{corr} in NaCl solution were determined from the corresponding polarization curves by Tafel extrapolation method.

The electrochemical parameters involved in the polarization process of copper electrodes, including i_{corr} or i'_{corr} , corrosion potential (E_{corr}), together with values of IE for SAMs in each case, are listed in Table 1. From the table it can be observed that NDT yields the lowest corrosion current density among the thiol molecules studied. Further the corrosion inhibition efficiency can be given in the order

NDT > DT > BDMT

The corrosion protection ability of the SAM may originate from the non-conducting nature and hydrophobicity of the alkane/aromatic moiety in the densely packed monolayers of the thiols on copper surface. The former retards electron transfer across the electrode interface, and the latter provides an effective barrier against the intimate contact of water to the underlying copper surface.

Figures 4 and 5 show the Nyquist plots recorded in 0.5 M NaCl solution for bare copper and SAM modified copper substrates (obtained by immersion for two hours in toluene solution), respectively. From

Table 1 — Electrochemical parameters derived from the polarization curves

Sample	E_{corr} (mV)	i_{corr} ($\mu\text{A cm}^{-2}$)	IE (%)
Bare Cu	-251	2.41	--
DT 10 mM	-337	0.17	93
NDT 10mM	-225	0.03	99
BDMT 10 mM	-256	0.28	88

Fig. 4, the values of charge transfer resistance (R_t) and double layer capacitance (C_{dl}) for bare copper were calculated to be $2.01 \times 10^{-3} \Omega \text{ cm}^2$ and $1.54 \times 10^{-7} \text{ F cm}^{-2}$, respectively using "PowerSuit" impedance software.

The impedance spectra of SAM modified electrodes are quite different from those of the bare electrode. Bare copper corrodes easily in 0.5 M NaCl solution, which results in poorly defined semicircle with a small charge-transfer resistance. The diameter of capacitive loop was increased markedly after SAM modification of copper. The capacitive loop is attributed to the relaxation time constant of the charge-transfer resistance (R_t) whose value is approximately equal to the diameter of the capacitive

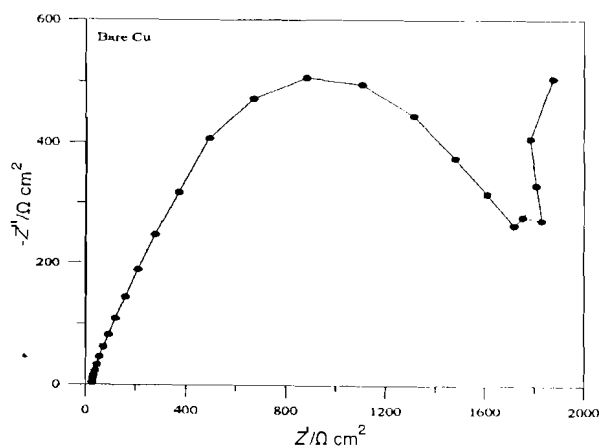


Fig. 4 — Nyquist impedance spectrum for the bare Cu electrode in 0.5 M NaCl solution at open circuit potential

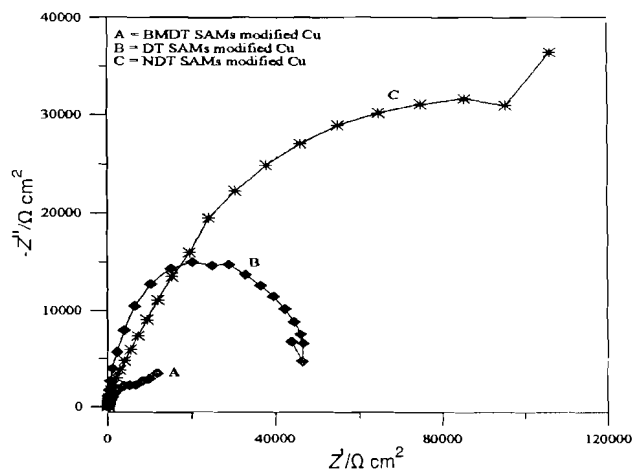


Fig. 5 — Nyquist impedance spectrum of DT, NDT and BDMT SAM modified Cu electrode in 0.5 M NaCl solution at open circuit potential. 10 mM solution of thiols in toluene was taken for SAM formation with a self-assembly period of 2 h

loop and the double-layer capacitance (C_{dl}) at the copper/electrolyte interface²⁵⁻²⁷, and the Warburg impedance (W) is due to diffusion of soluble reactant or product species²⁸. This indicates that the SAM film is relatively stable and can protect copper from corrosion in NaCl. However, at low frequencies, DT and BMDT SAM have shown deviation from regular semicircle. It may be due to penetration of SAM layer by electron and presence of molecule size defects in SAM even though they are defect free¹¹.

Fitted curves are plotted in term of the equivalent circuit shown in Fig. 6. Table 2 shows the charge-transfer resistance and capacitance values for bare and SAM modified copper. Accordingly the inhibition efficiency (IE) is calculated from the following formula

$$IE (\%) = (R'_t - R_t) (100)/R_t$$

where R'_t and R_t are the charge-transfer resistances for the Cu/SAM and bare Cu, respectively.

The inhibition efficiency observed by the impedance technique has a very good agreement with the IE values calculated using polarization technique (Table 1) within $\pm 5\%$ variation. Further, the results show that the corrosion resistance of the SAM is as follows:

$$NDT > DT > BDMT$$

which is also the trend noticed earlier from polarization measurements.

Effect of thiol concentration

The copper electrode was immersed in different thiol molecules of varying concentration in toluene solvent in order to find out the threshold concentration of thiol at which maximum inhibition efficiency is offered. For that thiol molecule concentration was varied from 0.1 to 20 mM and the copper electrodes were uniformly immersed in thiol solution for 2 h and then the SAM covered electrodes were evaluated using potentiodynamic polarization technique. Table 3 shows the electrochemical parameters derived from the polarization curves.

It is observed from this table that in general, the corrosion current density values are reduced drastically as the concentration of thiol increases from 0.1 to 20 mM. The protection ability of NDT SAM against copper corrosion shows a maximum efficiency of 99% at 10 mM concentration. The DT SAM exhibits a maximum efficiency of 93% at 10 mM concentration. Like DT and NDT SAM, the

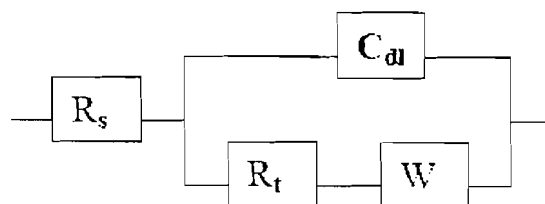


Fig. 6 — Equivalent circuit for AC impedance spectra

Table 2 — Electrochemical parameters obtained from fitting of impedance data

Sample	R'_t ($\Omega \text{ cm}^2$)	C_{dl} ($\times 10^{-7}$)	IE (%)
Bare Cu	2011	1.54	--
DT 10 mM	47960	0.003	96
NDT 10mM	157367	0.0003	99
BDMT 10mM	12658	0.040	84

Table 3 — Effect of thiol concentration

Thiol conc. (mM)	E_{corr} (mV)	i_{corr} ($\mu\text{A}\cdot\text{cm}^{-2}$)	IE %
Bare Cu	-251	2.41	---
Cu/DT			
0.1	-285	0.31	87
1.0	-326	0.19	92
2.5	-273	0.19	92
5	-346	0.18	93
10	-337	0.17	93
20	-208	0.14	94
Cu/NDT			
0.1	-236	0.30	88
0.5	-231	0.19	92
1.0	-196	0.14	94
2.5	-203	0.05	98
10	-225	0.03	99
20	-240	0.01	99
Cu/BMDT			
0.1	-218	1.97	18
0.5	-207	0.35	86
1.0	-224	0.32	87
2.5	-199	0.31	87
5.0	-187	0.31	87
10	-256	0.28	88
20	-239	0.18	93

corrosion protection ability of BDMT SAM also increases with increase of its concentration but it is in the range of 84 to 93% only and even at the concentration of 20 mM.

Effect of immersion time

The duration of immersing the electrode in thiol solution, i.e., the time for self assembly, is expected to influence the extent of formation of the SAM on the copper surface and hence on the inhibition efficiency of the modified electrode. To find out the optimum immersion time at which maximum efficiency could be realized, the electrode was immersed in toluene solution of thiol (10 mM) for different immersion times and then evaluated by potentiodynamic polarization studies in 0.5 M NaCl solution. Immersion time was varied from 15 to 1200 min and the experiments were repeated with the same concentration of the three thiols in toluene solution.

Table 4 shows that the inhibition efficiency generally increases with increase of time for self assembly and attains an *IE* of above 90% in about 2 h of immersion. This trend is well-noticed in the case of DT and BDMT, while with NDT inhibition efficiency reaches above 90% after 30 min of immersion. The self-assembly of NDT on copper takes place rapidly and within 30 min it attains almost a full monolayer coverage resulting in an *IE* of 96%. On the other hand, self assembly of DT and BMDT on copper is relatively less rapid and a minimum of about 2 h immersion time is needed to attain a near monolayer coverage.

Unlike DT, NDT and BMDT molecules have the choice of bonding with either of two terminals –SH groups onto the copper surface, which increase the probability of bond formation, resulting in the high rate of adsorption. The rate of absorption increases with concentration of thiol and immersion time which was reflected from inhibition efficiencies at various concentrations and immersion time. However, lower inhibition efficiency of BMDT SAM as compared to DT SAM may be due to its shorter chain length.

Effect of solvent

It was considered interesting to examine if the solvent used to prepare thiol solution had any effect on the property of the SAM formed. The role of solvent in self assembly process is to bring the thiol molecules into homogeneous solution phase facilitating smooth application on the substrate surface and subsequently get evaporated leaving the thiol molecule on the surface. The process of solvent

Table 4 — Effect of self-assembling time

Self assembling time (min)	E_{cor} (mV)	i_{cor} ($\mu\text{A}\cdot\text{cm}^{-2}$)	<i>IE</i> %
Cu	-251	2.41	--
Cu/DT			
15	-296	1.17	21
30	-339	0.93	62
60	-335	0.54	77
120	-337	0.17	93
300	-258	0.33	99
1200	-242	0.13	99
Cu/NDT			
15	-192	0.25	89
30	-226	0.11	95
45	-198	0.09	96
60	-254	0.08	97
90	-225	0.07	97
120	-239	0.07	97
300	-160	0.01	99
Cu/BMDT			
15	-233	2.27	6
30	-237	0.94	61
45	-230	0.45	81
60	-256	0.35	86
90	-226	0.19	92
120	-243	0.10	96
1200	-246	0.04	98

evaporation depends on the characteristics of the solvent. Hence it is likely that the solvent evaporation could have some influence on the characteristics of the monolayer formed. To look into this aspect, experiments were carried out using different solvents for solubilising the thiol compounds. Besides toluene, ethanol, dimethylformamide and acetonitrile were used in this study. An immersion time of two hours for SAM formation from the solution and a thiol concentration of 10 mM were employed. The SAM covered electrodes were then evaluated by potentiodynamic polarization measurements in 0.5 M NaCl solution and the results are given in Table 5.

It can be seen from Table 5 that the DT/SAM formed using DMF as a solvent gives better corrosion protection when compared to other solvents. Unfortunately, NDT is insoluble in DMF. In the case of NDT it shows a very high inhibition efficiency of 99% in toluene, which shows that it is a very good solvent for formation of monolayer.

Table 5 — Effect of solvent
Immersion time: 2 h; Thiol concentration: 10 mM

Solvent	E_{corr} (mV)	i_{corr} ($\mu\text{A cm}^{-2}$)	IE(%)
Bare Cu	-251	2.41	—
DT			
Toluene	-337	0.17	93
Ethanol	-288	0.07	97
DMF	-340	0.04	98
NDT			
Toluene	-225	0.03	99
Acetonitrile	-306	0.10	96
Ethanol	-263	0.04	98
BMDT			
Toluene	-256	0.28	88
Ethanol	-218	0.46	81
Acetonitrile	-263	0.28	88

The improved inhibition efficiency of SAM may be related to solubility of the DT in solvents. The solubility of all compounds is influenced by the possibility of H-bonding between solute and solvent. In the present case, the molecule of DMF and $\text{C}_2\text{H}_5\text{OH}$ can form two and one hydrogen bond, respectively, with DT whereas toluene does not have this feature. This leads to the solubility in the order of $\text{DMF} > \text{C}_2\text{H}_5\text{OH} > \text{toluene}$. Consequently, a good quality of SAM with better corrosion inhibition efficiency is formed rapidly by (DT + DMF) solution as compared to (DT + $\text{C}_2\text{H}_5\text{OH}$) solution. Thus, the adsorption process of DT on copper surface is very fast when DMF is used as a solvent.

Surface characterization of SAM modified copper surface

FT-IR reflection spectroscopy

The formation of SAMS on copper electrode surface was verified using infrared spectroscopy. Figures 7-9 show FTIR reflection spectrum of copper surface modified with DT, NDT and BDMT, respectively after over night self-assembly period in ethanolic solution.

Figure 7 shows the C–H region in the reflectance spectrum of DT covered on copper surface and the peaks at 2918 and 2848 cm^{-1} are the asymmetric and symmetric stretching of vibration of alkyl chain. The asymmetric CH_2 stretching vibration at 2918 cm^{-1} is a useful indicator for SAM of exceptional quality. The peaks at 2954 and 2878 cm^{-1} are assigned to

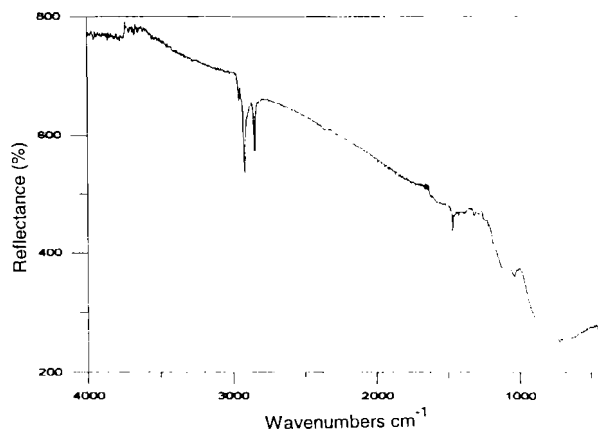


Fig. 7 — FT-IR reflection spectrum for DT/SAM on copper surface

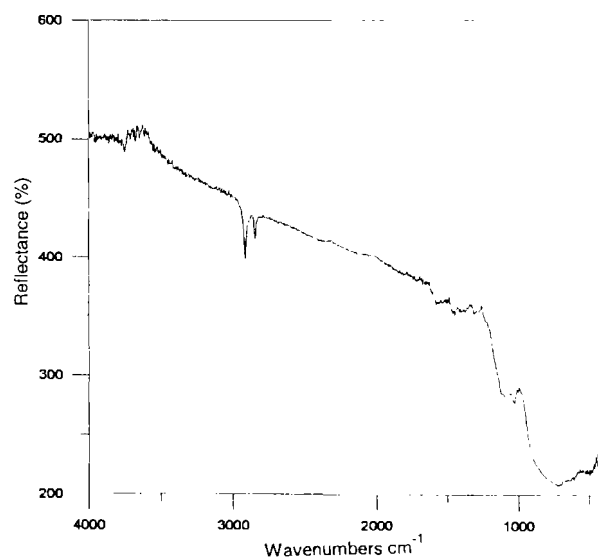


Fig. 8 — FT-IR reflection spectrum for NDT/SAM on copper surface

asymmetric (ν_a) and symmetric (ν_s) CH_3 modes, respectively. The IR spectrum does not show absorption around 2565 cm^{-1} corresponding to S–H bond stretching which indicates the formation of Cu–S bond between 1-decanthiol and copper surface.

Figure 8 shows the C–H region in the reflectance spectrum of NDT covered copper surface. The bands at 2917 and 2849 cm^{-1} are assigned to the asymmetric (ν_a) and symmetric (ν_s) CH_2 modes, respectively. One important distinguishing feature of IR spectra of NDT SAM vis-à-vis the DT SAM is the absence of peaks at 2954 and 2918 cm^{-1} due to the absence of $-\text{CH}_3$ functional group. The spectrum also does not show absorption peak corresponding to S–H bond.

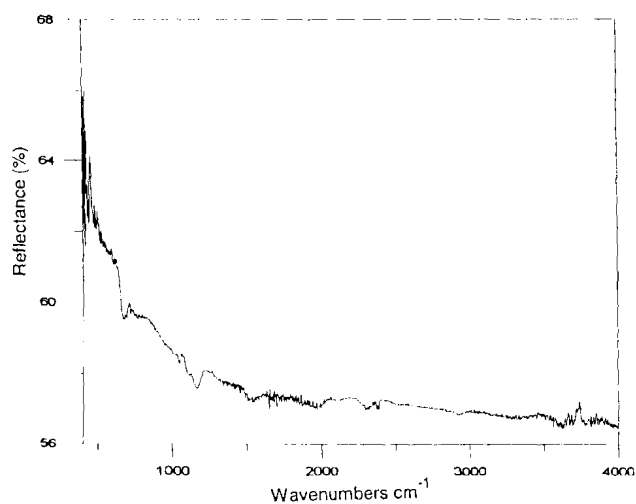


Fig. 9 — FT-IR reflection spectrum for BDMT/SAM on copper surface

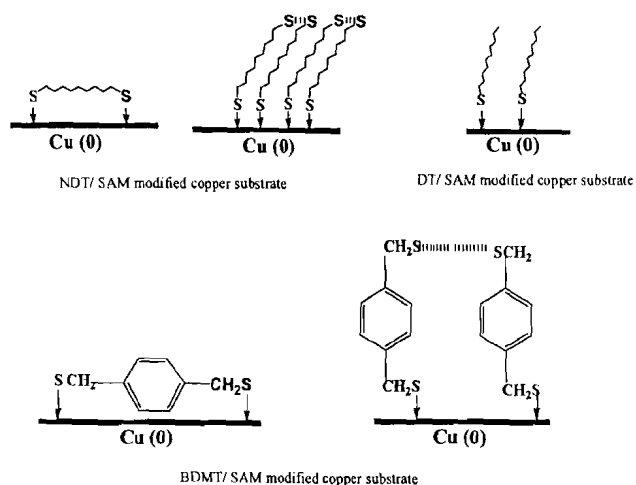


Fig. 10 — Self assembled monolayer of NDT, NDT and BDMT on oxide free copper substrate

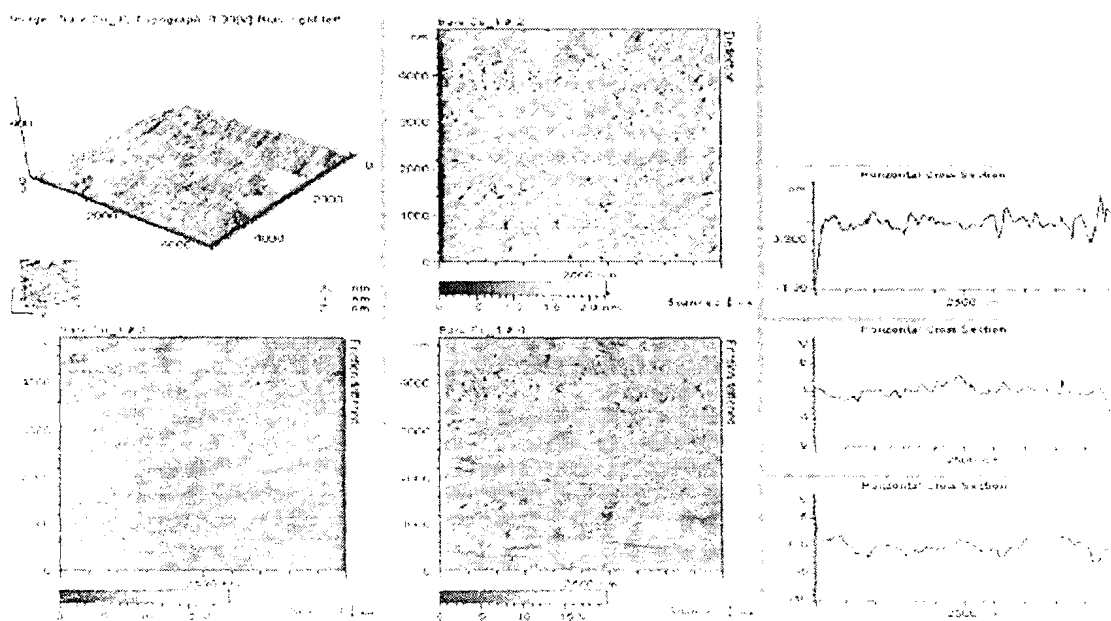


Fig. 11 — Typical topography (3-dimensional), deflection and friction images obtained for bare copper surface and their cross section analysis

The absence of S–H band in NDT may be due to the alignment of NDT molecule with its axis parallel to the copper surface or formation of disulphide bond between vertically aligned NDT with terminal SH group (Fig. 9). Figure 9 shows the IR spectra obtained for the BDMT/Cu. The peak at 681.51 cm^{-1} corresponds to the C–H stretching of 1,4-substituted benzene ring. The absorption at 1682, 1699 and 1170 cm^{-1} are the overtone and combination bands indicating ring substitution and ring hydrogen rocking vibration, respectively. The absence of S–H stretching

absorption at 2565 cm^{-1} is probably due to the linking of the BDMT molecules to Cu with both terminal –SH groups binding to the substrate. Alternatively, the possibility of formation of disulphide bond (S–S) between two vertically aligned adjacent BDMT molecules could also be visualized (Fig. 10)

Atomic force microscopy

Figure 11 shows the AFM images (Topography-3D, Deflection and Friction) of the bare and SAM modified copper surface. In the case of NDT

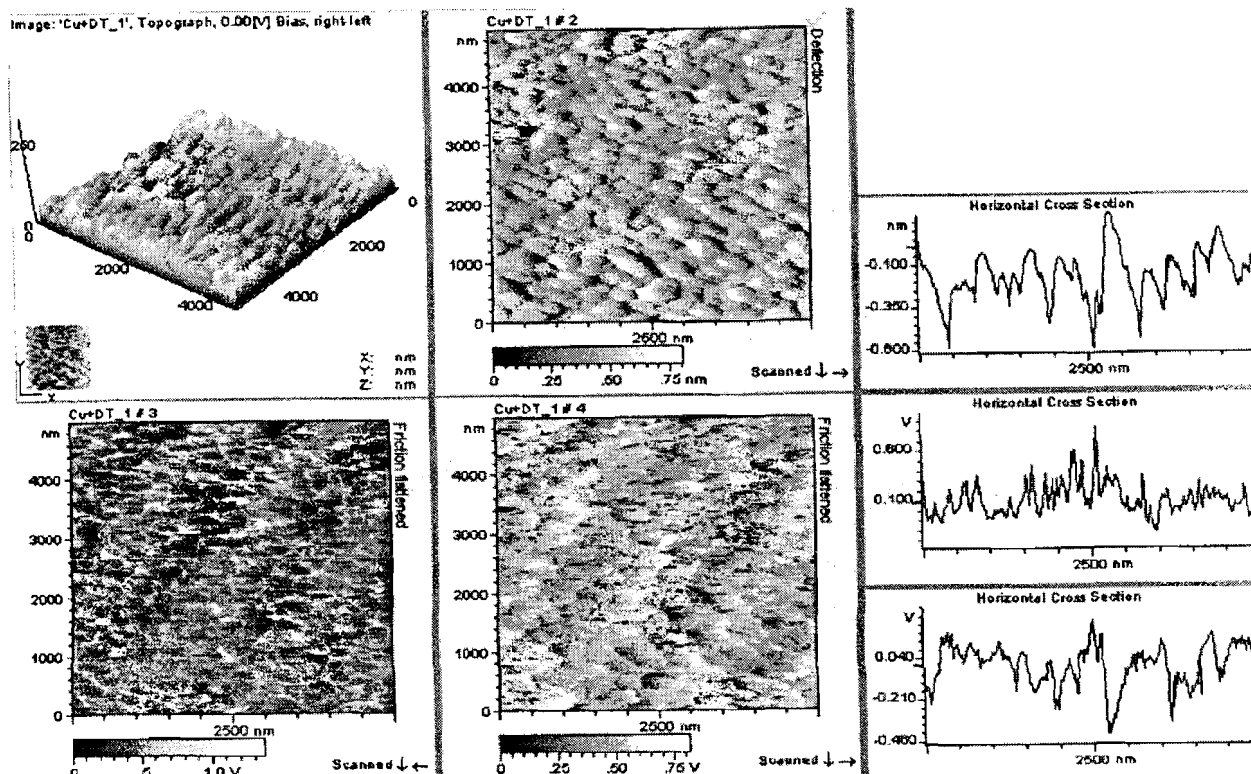


Fig. 12 — Typical topography (3-dimensional), deflection and friction images obtained for DT/SAM modified copper surface and their cross section analysis

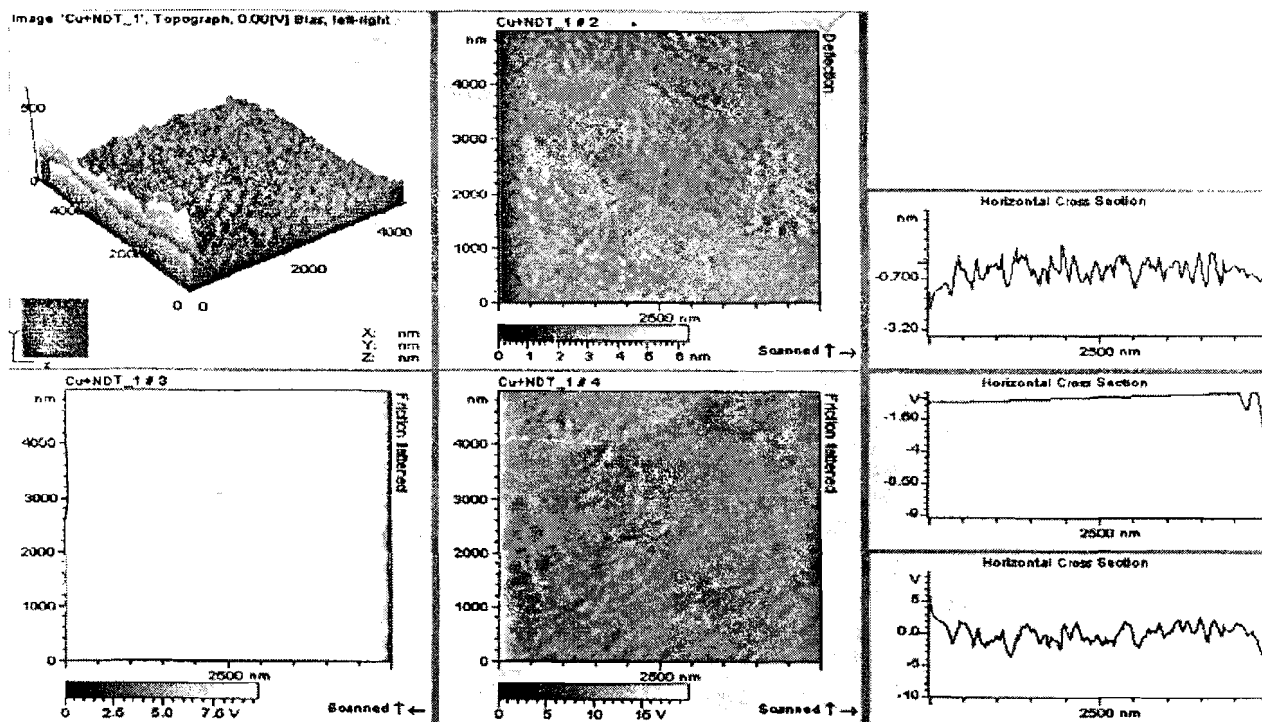


Fig. 13 — Typical topography (3-dimensional), deflection and friction images obtained for NDT/SAM modified copper surface and their cross section analysis

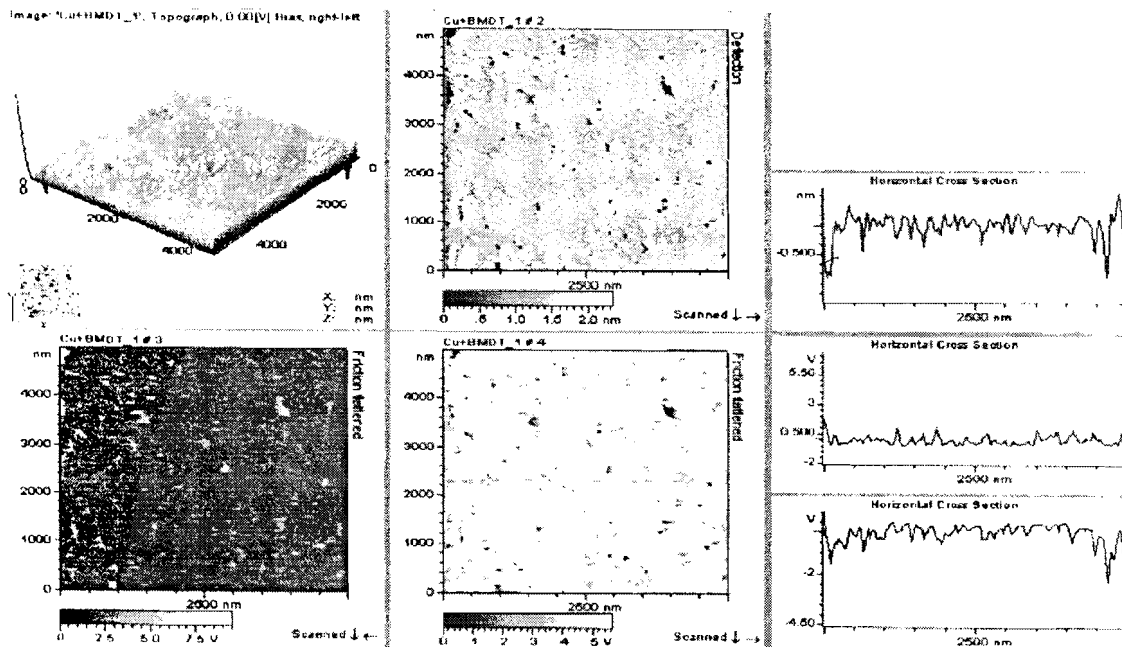


Fig. 14 — Typical topography (3-dimensional), deflection and friction images obtained for BMDT/SAM modified copper surface and their cross section analysis

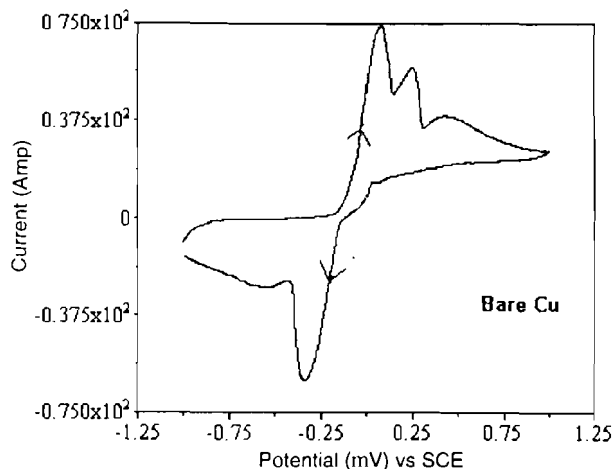


Fig.15 — Cyclic voltammogram of bare copper electrode in 0.5 M NaCl solution at a scan rate of 20 mVs^{-1}

(Figs 12-14), the formation of monolayer is uniform compact and dense. No defects or pinholes are observed. In BMDT (Fig. 14) modified electrodes, the SAM coverage was found to contain pinholes and defects even after a self assembly time of more than 24 h, which clearly indicates the absence of a complete monolayer coverage through SAM formation. The polarization results also show a relatively low inhibition efficiency values when compared to DT and NDT SAM.

Cyclic voltammetric studies

Cyclic voltammetry (CV) measurement were carried out at a scan rate of 20 mV/s in the potential rang of -0.80 to 0.80 V versus SCE in aqueous solution of 0.5 M NaCl . The cyclic voltammogram obtained on bare copper electrode obtained is shown in Fig. 15. During the forward scan they exhibited two oxidation peaks at 0.245 and 0.69 V and one large reduction peak at -0.33 V during the reverse scan.

Figure 16 shows the three CV curves of DT, NDT and BMDT SAM modified copper electrode, respectively. For SAM formation, 10 mM thiol solution (in toluene) was used with a self-assembly time of 2 h . In all the three cases, the second cycle exhibits distinctive polarization behaviour, giving very small anodic and cathodic peaks. When compared with bare copper, SAM-modified electrodes are showing decreased peak current. The peak current for anodic reaction is significantly decreased in the case of DT and NDT, whereas BMDT shows a appreciable amount of oxidation current during the forward scan. This can be attributed to the dissolution of copper through the pinholes of the film. The decrease in reduction peak current of SAM modified copper electrode may be due to the reduction of soluble CuCl_2^- complex and the CuCl layer formed on the copper surface¹².

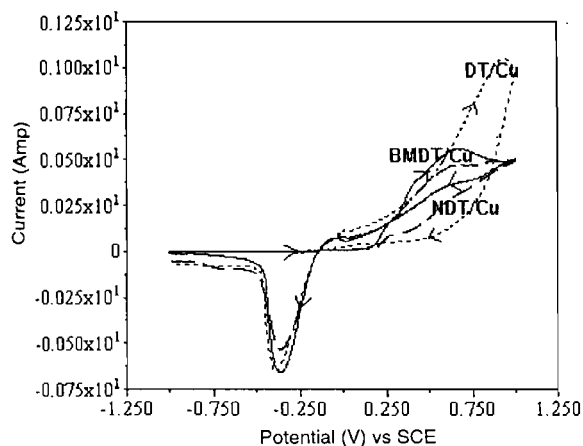


Fig. 16 — Cyclic voltammogram of BMDT, DT and NDT SAM modified copper electrode in 0.5 M NaCl solution at 20 $\text{mV}\cdot\text{s}^{-1}$ scan rate

Conclusion

The DT, NDT and BDMT displayed very strong corrosion protection ability to underlying copper substrate in NaCl solution.

- Thiol concentration and self assembly period markedly affect the quality of SAM on copper
- Solvent used for dissolving different thiol have only a marginal effect on the inhibition efficiency
- Under similar experimental conditions, corrosion resistance of the SAM is as follows $\text{NDT} > \text{DT} > \text{BDMT}$

References

- 1 Revie W R, *Uhlig's Corrosion Hand Book* (John Wiley and Sons Inc.), 2000.
- 2 Comizzoli R B, Frankenthal R P & Sinclair J D, *Corrosion Engineering of Electronic and Photonic Devices: Corrosion and Environmental Degradation, Vol. 19, Materials Science and Technology series* (Wiley-VCH, Weinheim, Germany).
- 3 Ulman A, *Chem Rev*, 96 (1996) 1533.
- 4 Laibins P E & Whitesides, *J Am Chem Soc*, 117 (1995) 12009.
- 5 Nuzzo R G & Allara D L, *J Am Chem Soc*, 105 (1983) 4481.
- 6 Maegle I, Jaehne E, Henke A, Adler H J P, Bram C, Jung C & Stratmann M, *Prog Org Coat*, 34 (1998) 1.
- 7 Ishibashi M, Itoh M, Nishihara H & Aramaki K, *Electrochim Acta*, 41 (1996) 241.
- 8 Jennings G K & Laibinis P E, *Colloids and Surfaces A-Physicochemical and Engineering Aspects*, 116 (1996) 105.
- 9 Jennings G K, Munro J C, Yong T S & Laibinis P E, *Langmuir*, 14 (1998) 6130.
- 10 Zamborini F G, Campbell J K & Crooks R M, *Langmuir*, (1998) 640.
- 11 Azzaroni O, Cipollone M, Vela M E & Salvarezza R C, *Langmuir*, 17 (2001) 1483.
- 12 Ma H Y, Yang C, Yin B S, Li G Y & Chen S H, *Appl Surf Sci*, 218 (2003) 143.
- 13 Feng Y Q, Teo W K, Siow K S, Gao Z Q, Tan K L & Hsieh A K, *J Electrochem Soc*, 144 (1997) 55.
- 14 Haneda R, Nishihara H & Aramaki K, *J Electrochem Soc*, 145 (1998) 1856.
- 15 Tremont R, Dejesuscardona H, Garciaorozco J, Castro R J & Cabrera C R, *J Appl Electrochem*, 30 (2000) 737.
- 16 Taneichi D, Haneda R & Aramaki K, *Corros Sci*, 43 (2001) 1589.
- 17 Li S L, Wang Y G, Chen S H, Yu R, Lei S B, Ma H Y & Liu D X, *Corros Sci*, 41 (1999) 1769.
- 18 Quan Z L, Chen S H & Li S L, *Corros Sci*, 43 (2001) 1071.
- 19 Wang C T, Chen S H, Ma H Y, Hua L & Wang N X, *J Serb Chem Soc*, 67 (2002) 685.
- 20 Tan Y S, Srinivasan M P, Pehkonen S O & Chooi S Y M, *Corros Sci*, 48 (2006) 840.
- 21 Benedetti A V, Sumodjo P T A, Nobe K, Cabot P L & Proud W G, *Electrochim Acta*, 40 (1995) 2657.
- 22 Tromans D & Sun R-H, *J Electrochem Soc*, 138 (1991) 3235.
- 23 Lee H P & Nobe K, *J Electrochem Soc*, 133 (1986) 2035.
- 24 Bacarella L & Griess J C Jr., *J Electrochem Soc*, 120 (1973) 459.
- 25 Feng Y, Teo W-K, Siow K-S, Gao Z, Tan K-L & Hsieh A-K, *J Electrochem Soc*, 144 (1997) 55.
- 26 Ma H, Cheng X, Li G, Chen S, Quan Z, Zhao S & Niu L, *Corros Sci*, 42 (2000) 1669.
- 27 Barcia O E & Matoos O R, *Electrochim Acta*, 35 (1990) 1601
- 28 Ma H, Chen S, Niu L, Shang S, Zhao S, Li S & Quan Z, *J Electrochem Soc*, 148 (2001) B208.